Active and Deformable Organic Electronic Devices based on Conductive Shape Memory Polyimide

Xinzuo Huang, Fenghua Zhang, Yanju Liu, and Jinsong Leng*

Cite This: *ACS Appl. Mater. Interfaces* 2020, 12, 23236−23243

Read Online

ACCESS | Metrics & More | Article Recommendations | SI Supporting Information

ABSTRACT: Smart, deformable, and transparent electrodes are a significant part of flexible optoelectronic devices. In this work, a novel approach to making highly transparent, smooth, and conductive shape memory polyimide hybrids has been proposed. Colorless shape memory polyimide (CSMPI) with high optical transparency and high heat resistance is served as the substrate for flexible electronic devices for the first time. A hybrid (Au/Ag) metal grid electrode embedded in CSMPI (BMG/CSMPI) is first fabricated via self-cracking template and solution-coating, the advantages of which include ultrasmooth surface, superior mechanical flexibility and durability, strong surface adhesion, and excellent chemical stability due to the unique embedded hybrid structure. The resulting white polymer light emitting diodes (WPLEDs) based on BMG/CSMPI with shape memory effect are active and deformable, and are converted from 2D device into 3D devices depending on its variable stiffness characteristics. The deformed 3D devices could actively recover to the original shape upon heating. Furthermore, ultrathin and flexible 3D optoelectronic devices fabricated using shape memory polymers can promote the development of advanced optoelectronic applications in the future.

KEYWORDS: *metal grid, flexible transparent electrodes, shape memory polyimide, organic light-emitting diodes, shape-changing devices*
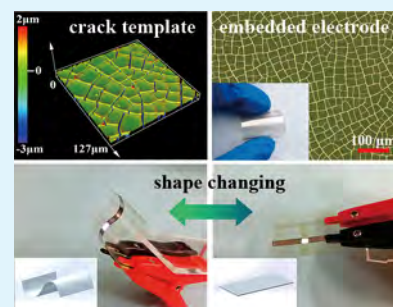
INTRODUCTION

Transparent electrodes (TEs) are a vital part of modern optoelectronic devices including organic light-emitting diodes (OLEDs),[1,2] solar cells, and[3,4] touch-screen displays.[5,6] As the linchpin of conventional TEs, indium tin oxide (ITO) is irreplaceable in optoelectronic devices by virtue of its balanced optical transmittance and excellent electrical conductivity.[7,8] However, the scarcity of indium leads to a high cost and expensive manufacturing processes. In addition, the brittle nature greatly limits its promotion in flexible optoelectronic devices, because ITO is prone to cracking under certain deformation stresses leading to performance degradation and device failure.[8,9] Next-generation applications will increasingly favor optoelectronic devices are that are lightweight, ultrathin, and flexible. This will require electrode materials suitable for mass manufacture with sufficient conductivity, transparency, and mechanical flexibility.[10] In recent years, many researchers have focused on searching for alternative TEs that can replace ITO in flexible devices. At present, three kinds of ITO alternatives have been reported, namely carbon based TEs[1,6,10] (carbon nanotubes, graphene, and conducting polymers), metal based TEs[11−13] (metal nanowires, metal grid, and ultrathin metal) and hybrid structure TEs[14−16] (a combination of carbon and metal-based TEs).

Metal grid is a significant contender for flexible TEs that can replace ITO in future flexible optoelectronic applications. In 2014, ITO alternatives account for 11% of TEs market share, of which 71% is attributed to metal grid owing to its

outstanding electrical and optical properties.[17] Conventional grid patterning techniques that include photolithography, inkjet printing, nanoimprint lithography, and rolling mask lithography,[18−20] need expensive special equipment and complicated procedure. Recently, some cheap and simple techniques have been used to prepare metal grid electrodes, such as the bubble template, the coffee ring effect template,[21] and the self-cracking template.[22] The self-cracking template is formed by spin coating or spraying the crackle precursor on the target substrate surface. Krzysztof et al. used a self-cracking template to prepare the transparent metal grid electrode for the first time, and discussed the effect of spin-coating on the electrode morphology and performance.[22] Giridhar et al. produced large area transparent conducting electrodes using crackle lithography, the rod coating method can potentially be adopted for roll-to-roll processing as well.[23] Giridhar et al. fabricated a core−shell network of Au/MnO₂ through crackle template process, and the flexible supercapacitors with high storage capacity and high transmittance was manufactured.[24] The cracking process is spontaneously triggered by the stress concentration in the precursor film.[25] Commonly used crackle

© 2020 American Chemical Society

Scheme 1. Schematic Diagram of the Preparation of the Hybrid (Au/Ag) Metal Grid Embedded in Colorless Shape Memory Polyimide
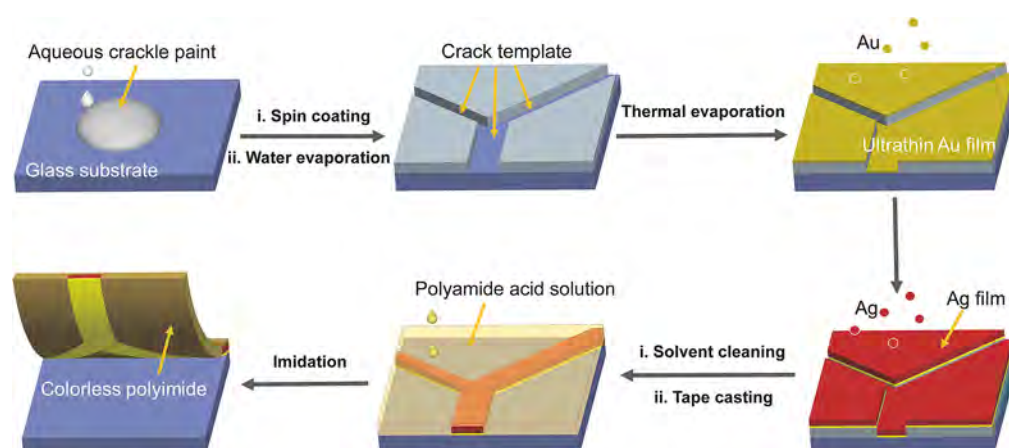
precursors include colloidal dispersions of TiO_2 or SiO_2 nanoparticles[22,26−29] and acrylic emulsions.[23,24,28,30] Transparent electrodes fabricated using self-cracking templates have been applied to flexible touch screen devices, capacitors and heaters. But many shortcomings still remain, such as high surface roughness, frail surface adhesion, poor chemical stability. We propose to use a solution-coating method to create the embedded metal grid in order to address the above drawbacks.

Shape memory polymers (SMPs) can memorize the temporary shape and recover to the original shape when exposed to external stimuli, including electric, light, microwave, pH, and heat.[31,32] The transparent shape memory polyacrylate with the glass transition temperature (T_g) lower than 120 °C have been used for flexible device, but the mechanical and optical properties could crucially deteriorate at high temperatures due to thermal instability.[33,34] In addition, implantable electronic devices such as microelectrode arrays and organic transistors prepared using SMP substrates have been reported.[35−37] Biomedical SMPs can bring shape reconfigurable and mechanically adaptive properties to implantable electronics, which can greatly reduce the injury associated with mechanical and geometrical mismatches brought about by surgical implantation. These biomedical SMPs all have a transition temperature near human body temperature (36 °C). Advanced optoelectronic devices have great demand for high thermal stability optical films. Therefore, we fabricated the colorless shape memory polyimide (CSMPI) with high transparency and thermal stability that could act as a substrate for active and deformable white polymer light emitting diodes (WPLEDs).[38]

In this work, we propose an innovative technique to manufacture a flexible metal grid transparent electrode. The uniform and controllable microcrack template is realized using cheap and eco-friendly aqueous crackle paint, the template fragments of which can be peeled off speedily. In addition, solution-coating methods have been used to fabricate a hybrid bilayered (Au/Ag) metal grid electrode embedded in CSMPI substrate. Ultrasmooth surface, superior mechanical flexibility and durability, strong surface adhesion and outstanding chemical stability were acquired owing to the particular embedded hybrid structure. Depending on the shape memory effect of polymer substrate, WPLEDs manufactured by this electrode can realize the shape changing from simple two-

dimensional (2D) device into the desired three-dimensional (3D) device relying on its variable stiffness characteristics. The deformed 3D devices could actively recover to the original shape upon heating. Therefore, this hybrid metal grid electrodes can be applied as a potential substitute for ITO to manufacture various ultrathin and flexible 3D optoelectronic devices in the future.

■ EXPERIMENTAL SECTION

Preparation of Metal Grid on Glass Substrate. The crackle paint was diluted to a concentration of 1−2 g mL^{-1} with deionized water. The paint films were formed on the glass substrate surface by spin coating at a rotation speed of 1000−2500 rpm. With the concentration kept constant, the spin coating rotation speed can be adjusted to control the paint film thickness. The faster the speed, the thinner the film thickness. The self-forming crack template was produced by drying the paint at constant temperature and humidity in a drying oven, the temperature was 25 °C and the humidity was 25% RH. Thermal evaporation was used to deposit Au and Ag film sequentially, the vacuum degree was ~10^{-4} Pa, and the evaporation rate was 0.5−1 nm/s, and a thickness meter (SQM160, INFICON) was used to precisely control the metal film thickness. The glass substrate covered with the metal film was ultrasonically cleaned in alcohol for 60 s. The hybrid bilayered (Au/Ag) metal grid on glass substrate was obtained following removal (by peeling) of the crack template.

Preparation of Metal Grid Embedded in CSMPI. The schematic diagram of synthesis of colorless shape memory polyimide (CSMPI) is shown in Suppoorting Information (SI) Scheme S1 TFDB (3.8 mmol), BPADA (4.0 mmol), and DMAc (20 mL) were added to the flask and stirred at room temperature to obtain the polyamic acid solution, which was casted onto the glass surface containing the metal grid. The stepwise imidization curing process (80−300 °C) was carried out, and the hybrid (Au/Ag) metal grid embedded in CSMPI was finally produced.

Preparation of Flexible 3D WPLEDs. Ultrasonic cleaned BMG/CSMPI was used as transparent anodes for the fabrication of white polymer light emitting diode. The device architecture was BMG/CSMPI/MoO_3 (2 nm)/PEDOT:PSS (30 nm)/ 0.5 wt % MEH-PPV:PFO (80 nm)/ Cs_2CO_3 (2 nm)/Al (150 nm). Both MoO_3, Cs_2CO_3 and Al films were formed by thermal evaporation. PEDOT:PSS was spin coated and baked at 150 °C for 20 min in air. The emissive polymer dissolved in toluene was spin coated and baked at 80 °C to remove the solvent.
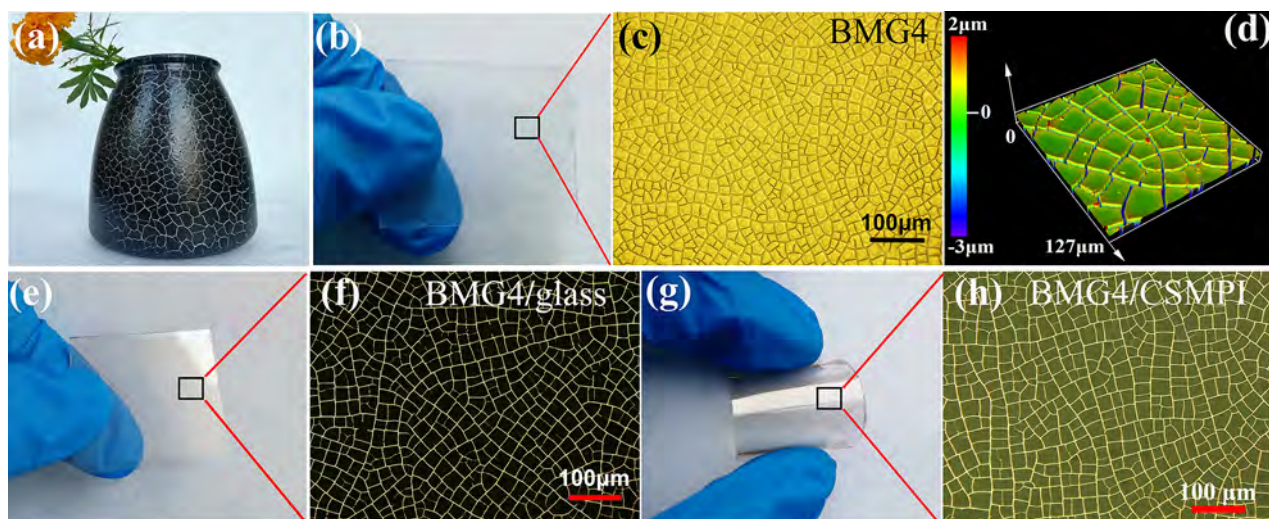
Figure 1. (a) Photo of vase sprayed with aqueous crackle paint. Photograph (b), optical microscopy image (c), and laser confocal micrograph (d) of the BMG4 crack template on glass substrate. Photograph (e) and optical microscopy image (f) of the metal grid on glass substrate. Photograph (g) and optical microscopy image (h) of the metal grid embedded in colorless shape memory polyimide.
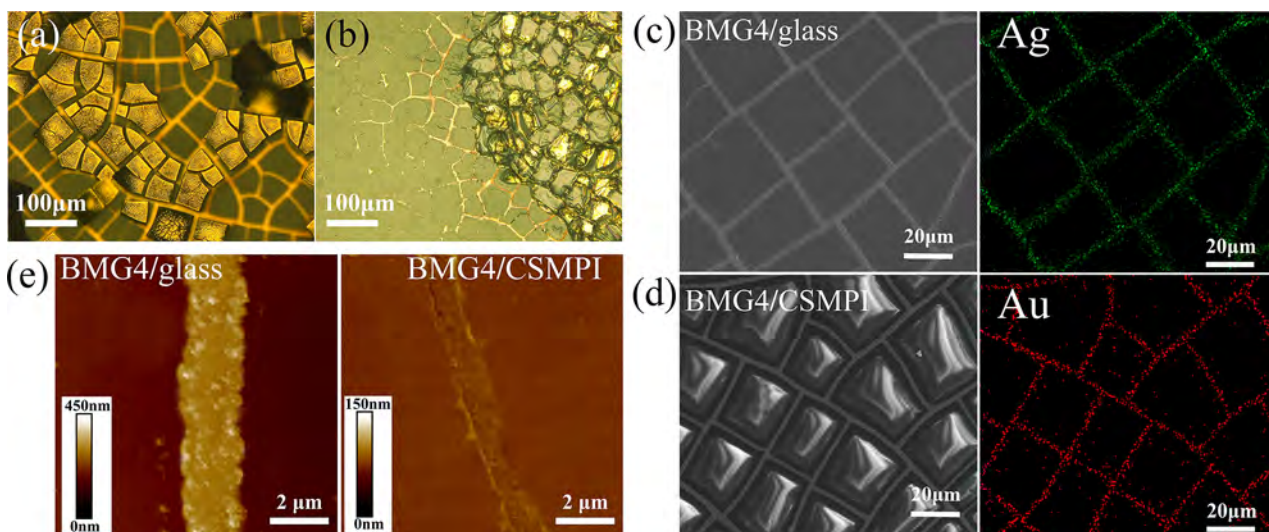
Figure 2. Optical microscopy image of (a) aqueous crackle paint and (b) acrylic emulsion during template removal process. (c) SEM image of BMG4/glass and the EDS mapping of Ag element on its surface. (d) SEM image of BMG4/CSMPI and the EDS mapping of Au element on its surface. (e) AFM pictures of hybrid metal grid on different substrates.

■ RESULTS AND DISCUSSION

The fabrication process of the hybrid bilayered (Au/Ag) metal grid embedded in colorless shape memory polyimide substrate (BMG/CSMPI) is illustrated in Scheme 1. First, the crack template is manufactured by spin coating aqueous crackle paint on glass substrate. Second, Au and Ag films are sequentially deposited onto the crack template by thermal evaporation. In the third step, the crack template is cleaned up by ultrasonic cleaning in ethanol while the hybrid metal grid remains on the glass substrate (BMG/glass). Finally, the polyamic acid solution is casted on the surface for thermal imidization, and the metal grid is embedded and transferred to CSMPI. All experimental parts could refer to the Supporting Information.

The aqueous crackle paint is widely applied in architectural and handicraft surface decoration due to its special texture, low cost, and eco-friendliness. Figure 1a shows a craft vase decorated with the aqueous crackle paint. The macroscopic crack paint texture is scaled down to the microscopic scale as a

template for the metal grid. The cracks emerge due to the concentration of internal stress in the paint film during the drying process.[39] At the same temperature, the different thicknesses of paint films lead to different water loss rates and internal stress states, and ultimately cause different crack morphologies. By controlling the thickness of paint films, we obtained four typical crack templates with different micro morphologies denoted as BMG1, BMG2, BMG3, and BMG4. Figure 1b demonstrates the picture of crackle paint film (BMG4) on glass substrate and the crack template is a transparent and uniform. Optical digital microscope images (Figure 1c and SI Figure S1a) and laser confocal microscope images (Figure 1d and SI Figure S1b) illustrate that the thinner the crack template, the more narrow and uniform are the cracks,[25] detailed data on the cracks are listed in SI Table S1. The crack width distribution of BMG4 is the most concentrated, with an average crack width of 2.3 μm. Under the condition of stable temperature and humidity, the
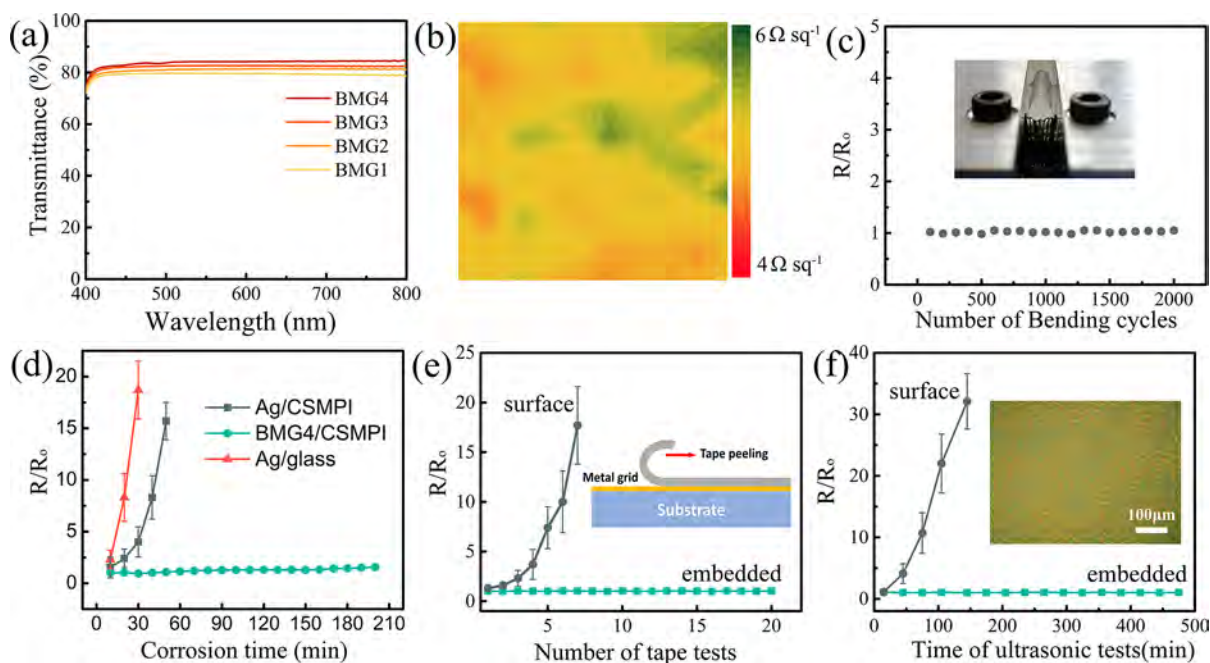
Figure 3. (a) The transmittance curves of BMG/CSMPI with different crack morphology. (b) Rs map over a 2.5× 2.5 cm² of BMG4/CSMPI. (c) Resistance variation over a large number of bending cycles, the inset picture shows the bending process. (d) Corrosion resistance test in HNO_3 solution (10 wt %). (e) Tape adhesion test results, the inset image shows the schematic of the tape tests. (f) The change of resistance after ultrasonic vibration (ethanol, 40 kHz), the inset image is optical microscopy image after 150 min ultrasonic vibration cleaning.

reproducibility of crack morphology can be guaranteed as long as the film thickness is controlled. Figure 1e is a photograph of the transparent metal grid on a glass substrate (BMG4/glass) following vacuum evaporation, the grid is highly transparent and has a metallic luster when observed with the naked eye. Optical microscopy images of BMG/glass prepared by different templates are shown in Figure 1f and SI Figure S1c, the metal grid has no defects as a result of the template removal process and remains completely intact. The morphology of BMG/glass is completely replicated in corresponding crack template. The results of hybrid metal grid embedded in polyimide are shown in Figure 1g and Figure 1h, BMG4/CSMPI is highly transparent and flexible, and the metal grid is completely transferred from the glass substrate surface to the flexible substrate. The crack template can be peeled off from the glass during the template removal process (Figure 2a), all fragments can be cleaned up within 60 s. General grid templates such as photoresists and acrylic emulsions are removed in the form of swelling and dissolution, which need more process time. In our previous experiments, we used acrylic emulsion as a crack template to prepare metal grid. However, when the acrylic template detaches through swelling and dissolution, it can damage the integrity of grids (Figure 2b). Because the absence of surface treatment on the glass substrate resulted in weak surface adhesion between the metal grid (Au/Ag) and the glass substrate. In order to prevent the metal grid from detaching during the acrylic template removal process, it is necessary to first deposit a thin chromium film as an intermediate layer to enhance the adhesion. However, the metal grid is more prone to breakage and defect when transferred from glass substrate to polyimide surface in the case of a chromium intermediate layer. This contradiction may lead to the fact that metal grids have not been reported to be transferred using the solution-coating method like Ag nanowires.[33] In this work, the unique and rapid

peeled-off of the crack template ensures that the metal grid can be transferred easily to flexible substrate without defect (Figure 1h).

Scanning electron microscope (SEM) images and corresponding energy dispersive spectrometer (EDS) mapping of hybrid metal grid on different substrates are shown in Figure 2. EDS mapping of BMG4/glass shows a metallic grid of Ag elements, because the Ag layer covers the bottom Au layer on the glass substrate (Figure 2c). EDS mapping of BMG4/CSMPI shows a metallic grid of Au elements, it illustrates that the original bottom Au layer is transferred to the surface, and the Ag layer is wrapped and protected by Au layer and polyimide substrate (as shown in Figure 2d). The BMG4/CSMPI cross-section has been is characterized using focused ion beam (FIB) and SEM. A platinum (Pt) protective coating prevents the metal grid layer from being destroyed by the ion beam. There is a good interface between the metal grid and the polymer substrate without obvious defects (SI Figure S2). Atom force microscopy images (AFM) of hybrid metal grid on different substrates are shown in Figure 2e. BMG4/glass is obviously protruded on the glass surface and has a large surface roughness (R_a = 63 nm). Moreover, BMG4/CSMPI is distinctly embedded in the flexible substrate with an ultrasmooth surface (R_a = 2.7 nm) that meets the requirement of OLEDs for low surface roughness. High surface roughness could cause shunted pathways and short circuit in OLEDs. The height profile curves of the metal grid on different substrates drawn by AFM is shown in SI Figure S3, which also shows that the surface of BMG4/CSMPI is smoother, and the thickness of metal grid can be calculated to be about 120−140 nm. X-ray photoelectron spectroscopy (XPS) was carried out to perform further component analysis in thickness direction of the hybrid metal grid (SI Figure S4). The BMG/glass is etched layer-by-layer and the element composition is analyzed at the same time. When the etch rate is constant, it can be inferred that the
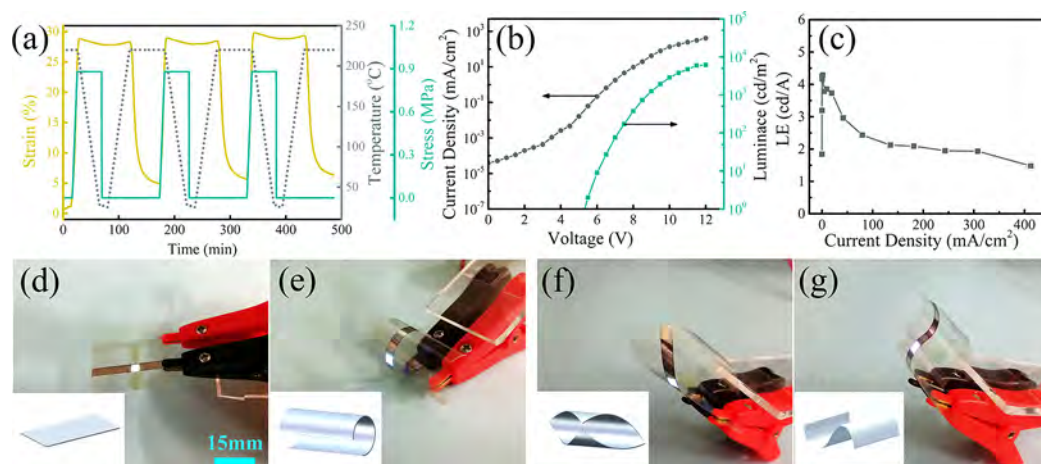
Figure 4. (a) Stretchable shape memory cycles of CSMPI substrate. (b) Current density–voltage-luminance characteristics of the WPLEDs fabricated with BMG4/CSMPI. (c) Luminance efficiency-current density characteristics of the WPLEDs. Photo of WPLEDs lighted at 8 V: (d) initial 2D planar device, (e,f) 3D cylindrical device after the shape is fixed; (g) 3D waved device with fixed shape.

thickness ratio of Au/Ag is about $^1/_3$, so the Ag layer is about 90−105 nm and the Au layer is about 30−35 nm. A cheaper metal network such as Ag, can be used as an electrical backbone, while the inert metal Au provides passivation protection and its work function matches WPLEDs. This bilayered hybrid structure is not only available for Au/Ag, but also can be extended to the compounding of any two other metals according to practical applications.

Figure 3a shows the transmittance curve in the visible range of a metal grid with different crack morphologies. The metal grid with narrower average grid width has higher transmittance, and the transmittance at 550 nm (T_{550}) of BMG4/CSMPI is 85%, meeting the requirement of the WPLEDs for transmittance of the electrode. It may be that the smaller fill factor of the narrow metal grid leads to a slight increase in light transmittance.[40] The four-point probe measurement test indicates that the narrower metal grid can also cause a decrease in conductivity (SI Table S1). Figure 4b shows that the square resistance (R_s) of BMG4/CSMPI is relatively uniform in spatial distribution (2.5 × 2.5 cm^2), and the average R_s is 5.2 Ω sq^{-1}. Figure of merit (FoM) is a reliable performance indicator to measure the quality and performance of TEs. In this work, eq 1 is used to calculate the FoM value,[41] where σ_{DC} and σ_{Opt} represent the direct current and optical conductivity, respectively. The calculation results reveal that BMG4/CSMPI has the highest FoM value of 428 (SI Table S1) and exceeds the FoM of commercial ITO electrodes. In addition, BMG4/CSMPI with the most uniform and narrowest grid can avoid the moire effect.[42,43] Therefore, we choose BMG4/CSMPI as transparent anode of WPLEDs for further study.

$$FoM = \frac{\sigma_{DC}}{\sigma_{Opt}} = \frac{188.5}{R_s \cdot (T_{550}^{-1/2} - 1)} \tag{1}$$

The bending cycle test suggests that BMG4/CSMPI has excellent mechanical flexibility and durability, and the conductivity remains stable after 2000 bending cycles (Figure 3c). The chemical stability of metal grid was tested by immersing them in HNO$_3$ solution (10 wt %) (Figure 3d). The chemical stability of the Ag grid on glass substrate (Ag/glass) is the worst. An Ag grid embedded on polyimide (Ag/CSMPI) is slightly more resistant to acid corrosion due to the

embedding. The embedded hybrid metal grid has the best chemical stability, because the unstable Ag layer is completely wrapped and protected by the Au layer and polymer substrate. Strong surface adhesion between electrodes and flexible substrates in flexible optoelectronic devices is necessary.[41] We used tape tests (using high-tack 3M Scotch tape) and ultrasonic vibration (ethanol, 40 kHz) to explore the surface adhesion of metal grids on different substrates.[44] The R_s for BMG4/glass increases after tape tests, and is 18 times higher after applying the test seven times (Figure 3e). Using ultrasonic vibration R_s for the BMG4/glass is 32 times higher after 150 min ultrasonic cleaning and there is large-scale detachment of the metal grid from the glass surface (Figure 3f). Results indicate that the surface adhesion of the metal grid on the glass surface is very weak; however, this weak adhesion ensures that the metal grid can be easily transferred to flexible substrate without defect. In contrast, the conductivity of BMG4/CSMPI is extremely stable after both 20 tape tests as well as ultrasonic vibration for more than 450 min (Figure 3e,f). The embedded structure endows the flexible metal grid with this ultrastrong surface adhesion. Therefore, the unique embedded hybrid structure makes the BMG4/CSMPI have superior mechanical flexibility and durability, strong surface adhesion and excellent chemical stability.

The T_g, storage modulus (E') and shape memory cycle performance of CSMPI were measured by dynamic thermomechanical analysis (DMA). CSMPI (T_g = 230 °C) possessed excellent shape memory effect because of huge difference in E' between glassy state (1.8 GPa) and rubber state (22 MPa) (SI Figure S5). The networks in shape memory polyimide can be characterized as macromolecular chain segments (reversible phase) and network points (stable phase). The netpoints link the macromolecular chain segments together, and these remain stable and determine the original shape of the polyimide. In CSMPI, a thermoplastic polymer, the physical cross-linking formed by intermolecular interactions serve as netpoints. Moreover, the flexible ether bonds lead to greater entanglement of the polyimide molecular chains, and more physical cross-linking points are formed as a result, which is beneficial to the shape memory effect. Shape memory cycle testing in tensile mode reveals that both the average shape recovery rate (R_r) and shape fixity rate (R_f) exceed 98%, and CSMPI has stable shape memory cycle performance (Figure 4a). The

recovery rate of the first cycle is lower, which may be caused by the residual strain resulting from the processing history.

WPLEDs based on solution-processing technologies show potential in energy-efficient lighting sources due to their low cost and their capacity for large-area fabrication.[45] OLEDs require anode materials with high work function, as this can improve the efficiency of hole injection and leads to better energy level matching for the device. BMG4/CSMPI can serve as a flexible transparent substrate for WPLED anodes and by using an embedded metal grid with Au as the surface metal a high work function (5.1 eV) is assured. Ultrasmooth metal grids can protect the WPLEDs from short circuits or shunts. And the strong surface adhesion of BMG4/CSMPI promotes mechanical stability and robustness of electronic cricuits. Flexible WPLEDs based on BMG4/CSMPI were fabricated using the following device architecture: BMG4/CSMPI/ MoO_3/PEDOT:PSS/0.5 wt % MEH-PPV:PFO/Cs_2CO_3/Al. In addition to acting as a hole injection layer, MoO_3 film also improves the hydrophilicity of the metal grid surface, which is beneficial for spin coating of PEDOT:PSS.[46] The characteristic properties of the device can be seen in Figure 4b and Figure 4c, the turn on voltage with luminance of 1 cd m^{-2} is 5.2 V, the maximum luminance efficiency (LE) is 4.3 cd A^{-1}. This is similar to the reported performance of devices fabricated on an ITO-coated glass substrate.[45,47] At present, all the fabrication process of OLEDs, including evaporation, spin coating, and so on, require that the substrate of device must be planar. Flexible OLEDs also adopt a 2D planar morphology in the initial undeformed state (Figure 4d), but depending on the variable stiffness characteristics of the shape memory polymer substrate, 2D planar WPLEDs can be converted into a variety of 3D morphologies, including cylindrical devices (Figure 4e and Figure 4f) and wave-liked devices (Figure 4g). Moreover, we demonstrated the shape recovery performance of 3D OLED devices. For example, the cylindrical device can quickly recover to the initial planar shape on the hot plate within 18 s (SI Figure S6). OLEDs based on BMG4/CSMPI therefore have potential to act as ultrathin and flexible 3D lighting fixtures in the future. In addition, BMG4/CSMPI is also applied to other flexible organic optoelectronic devices, such as flexible organic solar cells and touch screens, etc.

CONCLUSIONS

In summary, hybrid bilayered (Au/Ag) metal grid electrodes embedded in colorless shape memory polyimide have been developed and used as substrates for fabrication of flexible shape memory 3D OLEDs. The electrode fabrication process is simple and low cost and merely requires preparation of a microcrack template using commercial aqueous crackle paint followed by rapid fragment removal within 60 s. BMG4/ CSMPI presents a sheet resistance of 5.2 Ω sq^{-1} at a transmittance of 85% (550 nm).The turn on voltage and maximum LE of the flexible WPLEDs based on BMG4/ CSMPI are 5.2 V and 4.3 cd A^{-1}, respectively. By making use of the variable stiffness characteristics of the shape memory polyimide, the WPLEDs can be converted from a 2D planar state into complex 3D structures. Most importantly, the 3D electronics devices are active and deformable, its shape can be fixed and recovered as desired. Flexible 3D electronic devices play an increasingly significant role in our daily life and are an active area of scientific research. Shape memory polyimide-based flexible 3D electronic devices display novel properties and have the robustness to withstand harsh environments. The present research points a new strategy for smart, flexible organic optoelectronic devices with active deformation in the future.

ASSOCIATED CONTENT

Ⓢ Supporting Information

The Supporting Information is available free of charge at https://pubs.acs.org/doi/10.1021/acsami.0c04635.

Details of materials used; characterization methods; supplementary figures and tables (PDF)

AUTHOR INFORMATION

Corresponding Author

Jinsong Leng − *National Key Laboratory of Science and Technology on Advanced Composites in Special Environments, Harbin Institute of Technology (HIT), Harbin 150080, PR China;* ⓘ orcid.org/0000-0001-5098-9871; Email: lengjs@ hit.edu.cn

Authors

Xinzuo Huang − *National Key Laboratory of Science and Technology on Advanced Composites in Special Environments, Harbin Institute of Technology (HIT), Harbin 150080, PR China*

Fenghua Zhang − *National Key Laboratory of Science and Technology on Advanced Composites in Special Environments, Harbin Institute of Technology (HIT), Harbin 150080, PR China*

Yanju Liu − *Department of Astronautical Science and Mechanics, Harbin Institute of Technology (HIT), Harbin 150001, PR China*

Complete contact information is available at: https://pubs.acs.org/10.1021/acsami.0c04635

Author Contributions

The manuscript was written through contributions of all authors. All authors have given approval to the final version of the manuscript.

Notes

The authors declare no competing financial interest.

ACKNOWLEDGMENTS

REFERENCES

(1) Han, T. H.; Lee, Y.; Choi, M. R.; Woo, S. H.; Bae, S. H.; Hong, B. H.; Ahn, J. H.; Lee, T. W. Extremely Efficient Flexible Organic Light-emitting Diodes with Modified Graphene Anode. *Nat. Photonics* **2012**, *6*, 105−110.

(2) Zhang, D.; Ryu, K.; Liu, X.; Polikarpov, E.; Ly, J.; Tompson, M. E.; Zhou, C. Transparent, Conductive, and Flexible Carbon Nanotube Films and Their Application in Organic Light-emitting Diodes. *Nano Lett.* **2006**, *6*, 1880−1886.

(3) Chun-Chao, C.; Letian, D.; Rui, Z.; Choong-Heui, C.; Tze-Bin, S.; Bing, Z. Y.; Steve, H.; Gang, L.; Weiss, P. S.; Yang, Y. Visibly Transparent Polymer Solar Cells Produced by Solution Processing. *ACS Nano* **2012**, *6*, 7185−7190.

(4) Gao, J.; Sun, T.; Giersig, M.; Kempa, K.; Pei, K.; Wang, Y.; Zhang, L.; Peng, W.; Lin, Q.; Ren, Z. Transparent Nanowire Network Electrode for Textured Semiconductors. *Small* **2013**, *9*, 733−737.

(5) Blake, P.; Brimicombe, P. D.; Nair, R. R.; Booth, T. J.; Jiang, D.; Schedin, F.; Ponomarenko, L. A.; Morozov, S. V.; Gleeson, H. F.; Hill,

E. W. Graphene-Based Liquid Crystal Device. *Nano Lett.* **2008**, *8*, 1704−1708.

(6) Sukang, B.; Hyeongkeun, K.; Youngbin, L.; Xiangfan, X.; Jae-Sung, P.; Yi, Z.; Jayakumar, B.; Tian, L.; Hye Ri, K.; Young Il, S. Roll-To-Roll Production of 30-Inch Graphene Films for Transparent Electrodes. *Nat. Nanotechnol.* **2010**, *5*, 574−578.

(7) Akshay, K.; Chongwu, Z. The Race to Replace Tin-Doped Indium Oxide: Which Material Will Win? *ACS Nano* **2010**, *4*, 11−14.

(8) Ellmer, K. Past Achievements and Future Challenges in The Development of Optically Transparent Electrodes. *Nat. Photonics* **2012**, *6*, 809−817.

(9) Sakamoto, K.; Kuwae, H.; Kobayashi, N.; Nobori, A.; Shoji, S.; Mizuno, J. Highly Flexible Transparent Electrodes Based on Mesh-Patterned Rigid Indium Tin Oxide. *Sci. Rep.* **2018**, *8*, 2825−283.

(10) Hecht, D. S.; Liangbing, H.; Glen, I. Emerging Transparent Electrodes Based on Thin Films of Carbon Nanotubes, Graphene, and Metallic Nanostructures. *Adv. Mater.* **2011**, *23*, 1482−1513.

(11) Spechler, J. A.; Koh, T.; Herb, J. T.; Rand, B. P.; Arnold, C. B. A Transparent, Smooth, Thermally Robust, Conductive Polyimide for Flexible Electronics. *Adv. Funct. Mater.* **2015**, *25*, 7428−7434.

(12) Paeng, D.; Yoo, J.; Yeo, J.; Lee, D.; Kim, E.; Ko, S. H.; Grigoropoulos, C. P. Low-Cost Facile Fabrication of Flexible Transparent Copper Electrodes by Nanosecond Laser Ablation. *Adv. Mater.* **2015**, *27*, 2762−2767.

(13) Stec, H. M.; Williams, R. J.; Jones, T. S.; Hatton, R. A. Ultrathin Transparent Au Electrodes for Organic Photovoltaics Fabricated Using a Mixed Mono-Molecular Nucleation Layer. *Adv. Funct. Mater.* **2011**, *21*, 1709−1716.

(14) Kholmanov, I. N.; Domingues, S. H.; Chou, H.; Wang, X.; Tan, C.; Kim, J.; Li, H.; Piner, R.; Zarbin, A. J. G.; Ruoff, R. S. Reduced Graphene Oxide/Copper Nanowire Hybrid Films as High-Performance Transparent Electrodes. *ACS Nano* **2013**, *7*, 1811−1816.

(15) Lee, M. S.; Lee, K.; Kim, S. Y.; Lee, H.; Park, J.; Choi, K. H.; Kim, H. K.; Kim, D. G.; Lee, D. Y.; Nam, S. High-performance, Transparent, and Stretchable Electrodes Using Graphene-metal Nanowire Hybrid Structures. *Nano Lett.* **2013**, *13*, 2814−2821.

(16) Kang, H.; Jung, S.; Jeong, S.; Kim, G.; Lee, K. Polymer-Metal Hybrid Transparent Electrodes for Flexible Electronics. *Nat. Commun.* **2015**, *6*, 6503−6510.

(17) Zhou, W.; Chen, J.; Li, Y.; Wang, D.; Chen, J.; Feng, X.; Huang, Z.; Liu, R.; Lin, X.; Zhang, H. Copper Mesh Templated by Breath-Figure Polymer Films as Flexible Transparent Electrodes for Organic Photovoltaic Devices. *ACS Appl. Mater. Interfaces* **2016**, *8*, 11122−11127.

(18) Zhong, Z.; Woo, K.; Kim, I.; Kim, H.; Ko, P.; Kang, D.; Kwon, S.; Kim, H.; Youn, H.; Moon, J. Defect-Free, Highly Uniform Washable Transparent Electrodes Induced by Selective Light Irradiation. *Small* **2018**, *14*, 1800676−1800684.

(19) Li, Y.; Meng, L.; Yang, Y. M.; Xu, G.; Hong, Z.; Chen, Q.; You, J.; Li, G.; Yang, Y.; Li, Y. High-Efficiency Robust Perovskite Solar Cells on Ultrathin Flexible Substrates. *Nat. Commun.* **2016**, *7*, 10214−10224.

(20) Kim, W. K.; Lee, S.; Hee, L. D.; Hee, P. I.; Seong, B. J.; Woo, L. T.; Kim, J. Y.; Hun, P. J.; Chan, C. Y.; Ryong, C. C. Cu Mesh for Flexible Transparent Conductive Electrodes. *Sci. Rep.* **2015**, *5*, 10715−10723.

(21) Michael, L.; Michael, G.; Oded, M.; Isaac, B.; Doron, A.; Shlomo, M. Transparent Conductive Coatings by Printing Coffee Ring Arrays Obtained at Room Temperature. *ACS Nano* **2009**, *3*, 3537−3542.

(22) Bing, H.; Ke, P.; Yuanlin, H.; Xiaojian, Z.; Qikun, R.; Qinggeng, L.; Yangfei, G.; Tianyi, S.; Chuanfei, G.; David, C. Uniform Self-Forming Metallic Network as A High-Performance Transparent Conductive Electrode. *Adv. Mater.* **2014**, *26*, 873−877.

(23) Rao, K. D. M.; Gupta, R.; Kulkarni, G. U. Fabrication of Large Area, High-Performance, Transparent, Conducting Electrodes Using a Spontaneously Formed Crackle Network as Template. *Adv. Mater. Interfaces* **2014**, *1*, 1400090.

(24) Kiruthika, S.; Sow, C.; Kulkarni, G. U. Transparent and Flexible Supercapacitors with Networked Electrodes. *Small* **2017**, *13*, 1701906.

(25) Lee, W. P.; Routh, A. F. Why Do Drying Films Crack? *Langmuir* **2004**, *20*, 9885−9888.

(26) Kiruthika, S.; Rao, K. D. M.; Kumar, A.; Gupta, R.; Kulkarni, G. U. Metal Wire Network Based Transparent Conducting Electrodes Fabricated Using Interconnected Crackled Layer as Template. *Mater. Res. Express* **2014**, *1*, 26301.

(27) Rao, K. D. M.; Kulkarni, G. U. A Highly Crystalline Single Au Wire Network as A High Temperature Transparent Heater. *Nanoscale* **2014**, *6*, 5645.

(28) Gupta, R.; Rao, K. D. M.; Srivastava, K.; Kumar, A.; Kiruthika, S.; Kulkarni, G. U. Spray Coating of Crack Templates for the Fabrication of Transparent Conductors and Heaters on Flat and Curved Surfaces. *ACS Appl. Mater. Interfaces* **2014**, *6*, 13688−13696.

(29) Kiruthika, S.; Gupta, R.; Kulkarni, G. U. Large Area Defrosting Windows Based on Electrothermal Heating of Highly Conducting and Transmitting Ag Wire Mesh. *RSC Adv.* **2014**, *4*, 49745−49751.

(30) Gupta, R.; Rao, K. D. M.; Kulkarni, G. U. Transparent and Flexible Capacitor Fabricated Using A Metal Wire Network as A Transparent Conducting Electrode. *RSC Adv.* **2014**, *4*, 31108−31112.

(31) Tong, M.; Liu, L.; Xin, L.; Liu, Y.; Leng, J. Shape Memory Polymers for Composites. *Compos. Sci. Technol.* **2018**, *160*, 169.

(32) Wang, W.; Liu, Y.; Leng, J. Recent Developments in Shape Memory Polymer Nanocomposites: Actuation Methods and Mechanisms. *Coord. Chem. Rev.* **2016**, *320−321*, 38−52.

(33) Yu, Z.; Zhang, Q.; Li, L.; Chen, Q.; Niu, X.; Liu, J.; Pei, Q. Highly Flexible Silver Nanowire Electrodes for Shape-Memory Polymer Light-Emitting Diodes. *Adv. Mater.* **2011**, *23*, 664−668.

(34) Gaj, M. P.; Wei, A.; Fuentes-Hernandez, C.; Zhang, Y.; Reit, R.; Voit, W.; Marder, S. R.; Kippelen, B. Organic Light-emitting Diodes on Shape Memory Polymer Substrates for Wearable Electronics. *Org. Electron.* **2015**, *25*, 151−155.

(35) Reeder, J.; Kaltenbrunner, M.; Ware, T.; Arreaga-Salas, D.; Avendano-Bolivar, A.; Yokota, T.; Inoue, Y.; Sekino, M.; Voit, W.; Sekitani, T.; et al. Mechanically Adaptive Organic Transistors for Implantable Electronics. *Adv. Mater.* **2014**, *26*, 4967−4973.

(36) Du, X.; Cui, H.; Sun, B.; Wang, J.; Zhao, Q.; Xia, K.; Wu, T.; Humayun, M. S. Photothermally Triggered Shape-Adaptable 3D Flexible Electronics. *Advanced Materials Technologies* **2017**, *2*, 1700120.

(37) Wang, J.; Zhao, Q.; Wang, Y.; Zeng, Q.; Wu, T.; Du, X. Self-Unfolding Flexible Microelectrode Arrays Based on Shape Memory Polymers. *Advanced Materials Technologies* **2019**, *4*, 1900566.

(38) Huang, X.; Zhang, F.; Liu, Y.; Leng, J. Flexible and Colorless Shape Memory Polyimide Films with High Visible Light Transmittance and High Transition Temperature. *Smart Mater. Struct.* **2019**, *28*, 55031.

(39) Yoshida, S.; Adachi, K. Numerical Analysis of Crack Generation in Saturated Deformable Soil under Row-planted Vegetation. *Geoderma* **2004**, *120*, 63−74.

(40) Rao, K. D. M.; Gupta, R.; Kulkarni, G. U. Fabrication of Large Area, High-Performance, Transparent Conducting Electrodes Using a Spontaneously Formed Crackle Network as Template. *Adv. Mater. Interfaces* **2014**, *1*, 1400090.

(41) Lee, H. B.; Jin, W. Y.; Ovhal, M. M.; Kumar, N.; Kang, J. W. Flexible Transparent Conducting Electrodes Based on Metal Mesh for Organic Optoelectronic Device Applications: A Review. *J. Mater. Chem. C* **2019**, *7*, 1087.

(42) Coe, J. V.; Heer, J. M.; Teeterskennedy, S.; Tian, H.; Rodriguez, K. R. Extraordinary Transmission of Metal Films with Arrays of Subwavelength Holes. *Annu. Rev. Phys. Chem.* **2008**, *59*, 179−202.

(43) Shin, D. K.; Park, J. Design of Moiré-free Metal Meshes Using Ray Tracing for Touch Screen Panels. *Displays* **2015**, *38*, 9−19.

(44) Chang, L.; Zhang, X.; Ding, Y.; Liu, H.; Liu, M.; Jiang, L. Ionogel/Copper Grid Composites for High-Performance, Ultra-Stable

Flexible Transparent Electrodes. *ACS Appl. Mater. Interfaces* **2018**, *10*, 29010−29018.

(45) Sun, Q.; Chang, D. W.; Dai, L.; Grote, J.; Naik, R. Multilayer White Polymer Light-Emitting Diodes with Deoxyribonucleic Acid-cetyltrimetylammonium Complex as A Hole-transporting/electron-blocking layer. *Appl. Phys. Lett.* **2008**, *92*, 251108.

(46) Hellstrom, S. L.; Vosgueritchian, M.; Stoltenberg, R. M.; Irfan, I.; Hammock, M.; Wang, Y. B.; Jia, C.; Guo, X.; Gao, Y.; Bao, Z. Strong and Stable Doping of Carbon Nanotubes and Graphene by MoOx for Transparent Electrodes. *Nano Lett.* **2012**, *12*, 3574−3580.

(47) Ho, G.; Meng, H.; Lin, S.; Horng, S.; Hsu, C.; Chen, L.; Chang, S. Efficient White Light Emission in Conjugated Polymer Homojunctions. *Appl. Phys. Lett.* **2004**, *85*, 4576−4578.